

Hopping Transport of Electrons in Dye-Sensitized Solar Cells

Juan Bisquert*

Departament de Física, Universitat Jaume I, 12071 Castelló, Spain

Received: September 14, 2007; In Final Form: October 17, 2007

A calculation of the chemical diffusion coefficient of electrons, D_n , in dye-sensitized solar cells, is presented, in the framework of the hopping model, where electron transport occurs by direct transitions between localized states in an exponential distribution. The Fermi-level dependence of D_n in the transport energy approximation is exactly the same as that in the multiple trapping model, but there are differences concerning the meaning of the parameters governing electron transport and the values of relevant energy levels inferred from experiments. The hopping model appears to describe well the experimental data of D_n from high-efficiency dye solar cells at various temperatures.

The subject of electron transport in nanostructured semiconductors surrounded by electrolytes has been amply studied, especially in relation to the characteristics of dye-sensitized solar cells (DSC).¹ The physical quantity of central interest is the chemical diffusion coefficient of electrons, D_n ,² which is measured by the common techniques such as intensity modulated photocurrent spectroscopy (IMPS), transient photocurrent under a small perturbation of the illumination, or impedance spectroscopy (IS).^{3,4} D_n has been reported as a function of Fermi level, E_F , in a large number of publications. However, significant uncertainties remain on the interpretation of the results that have an important impact on the wider topic of modeling and characterization of DSC devices.^{3–7}

Motivated by such problems, this paper proposes an alternative interpretation of $D_n(E_F)$ based on the hopping model for carrier transport in disordered solids,⁸ where electron displacement occurs by direct transitions via localized states.^{9–12} This is contrast to the widely used framework of multiple trapping (MT) where electron displacement takes place via extended states at the conduction band edge at E_0 , with the free electron diffusion coefficient, D_0 , being reduced to D_n by trapping–detrapping events.^{2,13} Here, we calculate $D_n(E_F)$ directly using the hopping model by integration of the jump frequency to the transport energy, E_T .¹² The calculation shows that D_n in hopping transport has a Fermi-level dependence *identical* to that in the MT model, as expected from the meaning of the transport energy concept.^{14–16} However, the interpretation of the microscopic parameters and temperature dependence in $D_n(E_F)$ is quite different. We compare the merits and limitations of both models using the experimental data of IS from high-efficiency DSC at different temperatures.⁵

Let us comment briefly on the main features of the MT model with localized states exponentially distributed in the energy scale and randomly distributed spatially.^{2,4} The distribution has the expression

$$g_L(E) = \frac{N_L}{k_B T_0} \exp[(E - E_0)/k_B T_0] \quad (1)$$

where k_B is Boltzmann's constant, N_L is the total density, and T_0 is a parameter with temperature units that determines the depth of the distribution. We assume that the temperature $T < T_0$. The carrier density in the localized states, n_L , is found as

$$n_L(E_F) = \int_{-\infty}^{E_0} g_L(E) f(E - E_F) dE \quad (2)$$

where $f(E - E_F)$ is the Fermi–Dirac function

$$f(E - E_F) = \frac{1}{1 + e^{(E - E_F)/k_B T}} \quad (3)$$

At room temperature, the chemical capacitance of the localized states is well described by the following expression¹⁷

$$C_\mu^L(E_F) = q^2 \frac{dn}{dE_F} = \frac{N_L q^2}{k_B T_0} \exp[-(E_0 - E_F)/k_B T_0] \quad (4)$$

where q is the positive elementary charge. Alternatively, the chemical capacitance of the extended states, with effective density N_0 , is

$$C_\mu^0(E_F) = \frac{q^2 n_0}{k_B T} = \frac{q^2 N_0}{k_B T} \exp[-(E_0 - E_F)/k_B T] \quad (5)$$

The total capacitance

$$C_\mu = C_\mu^0 + C_\mu^L \quad (6)$$

is shown in Figure 1a. It is observed that the slope is $1/k_B T_0$ when the Fermi level is deep in the band gap and changes to $1/k_B T$ when the Fermi level approaches the conduction band. The calculation of the chemical diffusion coefficient uses the equation²

* E-mail: bisquert@fca.uji.es.

$$D_n = \frac{C_\mu^0(E_F)}{C_\mu^0(E_F) + C_\mu^L(E_F)} D_0 \quad (7)$$

Therefore, $D_n \approx D_0$ (the free electrons diffusion coefficient) when the Fermi level is close to the conduction band and cancels the transient effects of the traps. Alternatively, when the Fermi level is deep we have from eq 7

$$D_n(E_F) = \frac{C_\mu^0}{C_\mu^L} D_0 = \frac{N_0 T_0}{N_L T} \exp\left[-(E_0 - E_F)\left(\frac{1}{k_B T} - \frac{1}{k_B T_0}\right)\right] D_0 \quad (8)$$

According to eq 8, the effect of trapping is described by a Fermi-level dependent prefactor that reduces the chemical diffusion coefficient with respect to D_0 . These results are illustrated in Figure 1b. The conductivity, σ_n , can be obtained from the generalized Einstein relation, which gives the expression⁴

$$\sigma_n(E_F) = D_n(E_F) C_\mu(E_F) \quad (9)$$

Equation 9 reduces to

$$\sigma_n = D_0 C_\mu^0(E_F) = \frac{q^2 N_0 D_0}{k_B T} \exp\left[-\frac{E_0 - E_F}{k_B T}\right] \quad (10)$$

Thus, σ_n depends only on the parameters of the free electrons, corresponding to the fact that in the MT model the traps do not affect the steady-state transport.⁴ Therefore, the slope of σ_n is $1/k_B T$ at all values of E_F , see Figure 1a.

Recently, this model has been applied extensively in DSC (for the multiple trapping regime in which $n_L \gg n_0$, i.e. $E_F \ll E_0$).^{3,4} We show in Figure 2 the experimental results of chemical capacitance and diffusion conductivity derived from IS measurement in ref 5 at different temperatures on a high-performance DSC formed with nanostructured TiO_2 and a I^-/I_3^- redox electrolyte. First, the chemical capacitance in Figure 2a shows the characteristic exponential dependence and is independent of temperature, confirming that the capacitance measures the DOS at the Fermi level as indicated in eq 4. In contrast to this, the conductivity in Figure 2b shows a strong dependence of temperature. This is because the conductivity is thermally activated as expected from eq 10, assuming that the free electron diffusion coefficient, D_0 , depends weakly on the temperature. In fact, the fits of Figure 2b to straight lines give values close to the thermal energies, $k_B T = 0.0236$ and 0.0288 eV at 273 and 333 K, respectively, in agreement with eq 10. The chemical diffusion coefficient, evaluated from C_μ and σ_n with eq 9, and shown in Figure 2c, obviously follows well the Fermi-level dependence indicated in eq 8, at the two measured temperatures.

These results show that the multiple trapping model gives a good description of electron transport in DSC, including the temperature-dependent features, as is agreed by many in the literature.¹³ Nonetheless, it must be remarked that the data in Figure 2c, and similar data in the literature, only give the raising part of the model in Figure 1b, and not the saturation to D_0 . Furthermore, D_0 has not been detected by any of the methods used in the literature to determine $D_n(E_F)$. So from the slope of the lines in Figure 2c, the only parameter that can be determined is T_0 . There are, therefore, important model parameters that cannot be extracted, namely, N_L , N_0 , E_0 , and D_0 . These are lumped in a prefactor in eq 8 and cannot be separated. This is

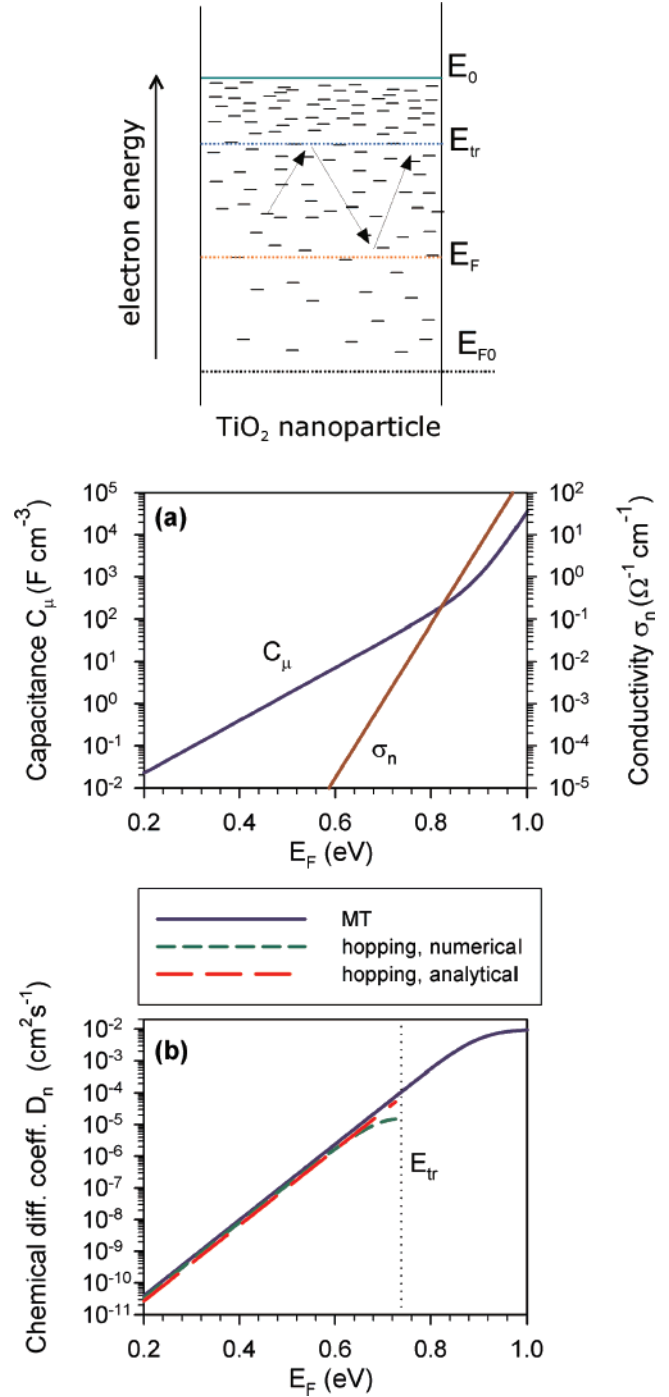


Figure 1. Scheme shows the trajectory for electron transport by hopping between localized states in the band gap: upward hops predominantly occur to the transport level (E_{tr}). Below is shown the representation of several quantities for charge accumulation and transport in an exponential DOS with the conduction band edge at the energy $E_0 = 1$ eV. E_F is the Fermi level potential. (a) Chemical capacitance and conductivity. (b) Chemical diffusion coefficient, calculated in multiple trapping approximation, and in the hopping model with the transport energy concept, both with the numerical integration of the average jump frequency, and with the analytical expression calculated in the text (eq 24). The following parameters were used in the calculation: $N_0 = 5.0 \times 10^{21}$ cm⁻³, $N_L = 10^{21}$ cm⁻³, $T = 275$ K, $T_0 = 800$ K, $D_0 = 10^{-2}$ cm²s⁻¹ (for multiple trapping), $\alpha = 0.5$ nm, and $\nu_0 = 5 \times 10^{12}$ s⁻¹ (for hopping transport).

a very significant problem that pervades the literature of DSC modeling because such parameters are needed to describe DSC operation.^{18,19}

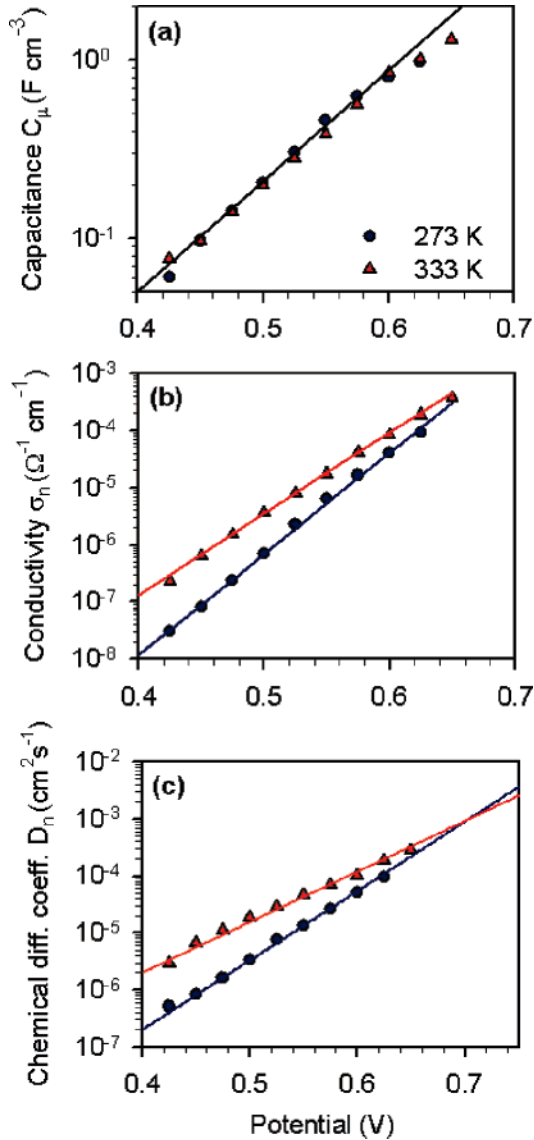


Figure 2. Representation of several quantities for charge accumulation and transport at different temperatures, in a high-efficiency (10.2%) DSC. The experimental points are the chemical capacitance C_μ and conductivity σ_n , which are obtained from IS data on capacitance and transport resistance reported in ref 5, using the cell area 0.18 cm² and active nanocrystalline TiO₂ electrode thickness 12 μ m. (a) Chemical capacitance. The fit line is $\ln C_\mu = -8.70 + V/0.0704$, corresponding to $T_0 = 808$ K. The carrier density is calculated with eq 50. (b) Electron conductivity. The fit lines are $\ln \sigma_n^{273K} = -34.6 + V/0.0245$, $\ln \sigma_n^{333K} = -28.9 + V/0.0306$. (c) Chemical diffusion coefficient D_n calculated with eq 9. The fit lines correspond to the hopping model with the transport energy concept, using the analytical expression in eq 24, and the fixed parameters $N_L = 10^{21}$ cm⁻³, $\alpha = 0.5$ nm, and $\nu_0 = 5 \times 10^{12}$ s⁻¹.

Another interesting observation in Figure 2c is the point of intercept of the lines at the different temperatures. According to eq 8, this marks the activationless transport at E_0 , that is, the position of the TiO₂ conduction band with respect to $E_{\text{redox}}(I^-/I_3^-)$.²⁰ However, the experimental value $E_0 \approx 0.7$ eV that is thus deduced from Figure 2c is clearly too low with respect to the values commonly admitted in the DSC area (0.9–1.0 eV).^{21,22} Therefore, the level for transport seems to be situated some 0.2 eV below the conduction band; this fact was already acknowledged in ref 6. Because this is not compatible with the standard formulation of the MT model, as described above, in the following we provide a description of the hopping model,

where this feature occurs by construction, and we calculate explicitly the chemical diffusion coefficient.

In the hopping model, the carriers move by direct transitions between the localized states of the distribution in eq 1.^{10,11} The transition probabilities are given by the upward and downward jump rates in the Miller–Abrahams²³ expression

$$\nu_1 = \nu_0 \exp\left[-2\frac{r}{\alpha} - \frac{E_j - E_i}{k_B T}\right] \quad (E_j > E_i) \quad (11)$$

$$\nu_1 = \nu_0 \exp\left[-2\frac{r}{\alpha}\right] \quad (E_j \leq E_i)$$

where ν_0 is the attempt-to-jump frequency, r is the distance between sites, α is the localization radius, and E_j and E_i are the energies of the target and starting sites, respectively. Under very general conditions, the chemical diffusion can be expressed in terms of the jump diffusion coefficient, D_J , and thermodynamic factor, χ_n , as^{4,24}

$$D_n = \chi_n D_J \quad (12)$$

The thermodynamic factor can be written

$$\chi_n = \frac{q^2 n}{k_B T C_\mu} \quad (13)$$

and for the distribution in eq 1 it has a constant value, $\chi_n = T_0/T$.² The jump diffusion coefficient can be expressed as^{4,24}

$$D_J = \langle \nu \rangle \langle r^2 \rangle \quad (14)$$

in terms of a mean effective jump frequency, $\langle \nu \rangle$, and the square of effective jump length, $\langle r^2 \rangle$. It was shown in previous work that in multiple trapping models eq 14 reduces to eq 7,² so that the chemical diffusion coefficient is readily obtained from the capacitances of free and localized states.

In the hopping model, we must obtain D_J by directly averaging the hopping rates of eq 11 over disordered spatial and energy configurations, taking into account the occupation established by the value of the Fermi level, in order to obtain the mean jump frequency $\langle \nu \rangle$. Because the hopping rates depend exponentially both on the energy difference and on the distance between pairs of sites, analytical calculation of such an average is usually very difficult, but it is partially simplified in a system with a steep distribution of localized states, where the hopping process is well described with the concept of transport energy.^{9,11} The rationale for such an approach is that in equilibrium the transport is governed by the fastest hop of a charge carrier. The most probable upward jump corresponds to an optimized combination of the distance and energy difference. Let $a = N_L^{-1/3}$ be the mean distance between localized sites. The average distance for states below any energy E_1 is

$$\langle r(E_1) \rangle = \left[\frac{4\pi}{3} \int_{-\infty}^{E_1} g(E) dE \right]^{-1/3} = \left(\frac{4\pi}{3} \right)^{-1/3} \exp\left(-\frac{E_1 - E_0}{3k_B T_0}\right) a \quad (15)$$

Inserting this average distance in eq 11, one can find the energy that optimizes the upward jump rate ν_1 . The result^{12,16} is that, independent of the energy of the starting site, the fastest hops occur toward sites in the vicinity of a specific level, the transport energy E_{tr} , as indicated in the scheme of Figure 1,

that is given by

$$E_{\text{tr}} = E_0 - \Delta E_{\text{tr}} \quad (16)$$

where

$$\Delta E_{\text{tr}} = 3k_{\text{B}}T_0 \ln \left[\frac{3\alpha T_0 (4\pi)^{1/3}}{2aT} \right] \quad (17)$$

The average jump distance is therefore evaluated by eq 15

$$\langle r(E_{\text{tr}}) \rangle = \frac{3T_0}{2T} \alpha \quad (18)$$

The jump frequency from the energy E to the transport energy is¹²

$$\nu(E, E_{\text{tr}}) = \nu_0 \exp \left(-2 \frac{\langle r(E_{\text{tr}}) \rangle}{\alpha} - \frac{E_{\text{tr}} - E}{k_{\text{B}}T} \right) \quad (19)$$

For the calculation of the jump diffusion coefficient, we average eq 19 as follows¹⁵

$$\langle \nu \rangle = \frac{1}{n_{\text{L}}} \int_{-\infty}^{E_{\text{tr}}} \nu(E, E_{\text{tr}}) g_{\text{L}}(E) f(E - E_{\text{F}}) dE \quad (20)$$

The main contributions arise from carriers between E_{F} and E_{tr} ; therefore, we can write

$$\langle \nu \rangle = \frac{1}{n_{\text{L}}} \int_{E_{\text{F}}}^{E_{\text{tr}}} \nu(E, E_{\text{tr}}) g_{\text{L}}(E) \exp[-(E - E_{\text{F}})/k_{\text{B}}T] dE \quad (21)$$

We calculate the carrier density below E_{tr} by using suitable approximations to the Fermi–Dirac distribution

$$n_{\text{L}} = \int_{-\infty}^{E_{\text{F}}} g(E) dE + \int_{E_{\text{F}}}^{E_{\text{tr}}} g(E) \exp[-(E - E_{\text{F}})/k_{\text{B}}T] dE = \frac{N_{\text{L}}}{1 - T/T_0} \exp \left(-\frac{E_0 - E_{\text{F}}}{k_{\text{B}}T_0} \right) \quad (22)$$

Calculating the integral in eq 21, we arrive at the result

$$\langle \nu \rangle = \nu_0 \left(1 - \frac{T}{T_0} \right) \exp \left[-3 \frac{T_0}{T} - (E_{\text{tr}} - E_{\text{F}}) \left(\frac{1}{k_{\text{B}}T} - \frac{1}{k_{\text{B}}T_0} \right) \right] \quad (23)$$

Therefore, the chemical diffusion coefficient is

$$D_{\text{n}} = \chi_{\text{n}} \langle r^2(E_{\text{tr}}) \rangle \langle \nu \rangle = \frac{9T_0^3}{4T^3} \left(1 - \frac{T}{T_0} \right) \exp \times \left[-3 \frac{T_0}{T} - (E_{\text{tr}} - E_{\text{F}}) \left(\frac{1}{k_{\text{B}}T} - \frac{1}{k_{\text{B}}T_0} \right) \right] \alpha^2 \nu_0 \quad (24)$$

Using eqs 9 and 4 we obtain the conductivity

$$\sigma_{\text{n}} = \frac{9N_{\text{L}}q^2T_0^2\alpha^2\nu_0}{4k_{\text{B}}T^3} \left(1 - \frac{T}{T_0} \right) \exp \times \left[-3 \frac{T_0}{T} - \frac{E_0 - E_{\text{tr}}}{k_{\text{B}}T_0} - \frac{E_{\text{tr}} - E_{\text{F}}}{k_{\text{B}}T} \right] \quad (25)$$

Let us remark on some features of these results. First of all, eqs 24 and 25 show the same Fermi-level dependence as that in MT, which is understandable because the transport has been

assumed to be governed by activated hops to E_{tr} . But there are important differences between the models. In the MT interpretation of electron transport in DSC, we usually adopt two essential parameters of the crystalline material: the free electrons diffusion coefficient, D_0 , and the conduction band edge, E_0 , that is the sole transport level. These parameters are independent of traps, and are needed separately to describe steady-state transport. In contrast, the hopping model lacks such parameters. The rate of transport is governed by the fundamental frequency ν_0 and the localization radius α , and the transport level E_{tr} is associated with the distribution of localized levels, depends on the temperature, and lies below E_0 .

Now we make an estimation of the values of D_{n} obtained in the framework of the hopping model using parameters from the literature: the total trap concentration $N_{\text{L}} = 10^{21} \text{ cm}^{-3}$, that is, $a = 1 \text{ nm}$,²⁵ the localization radius $\alpha = 0.5 \text{ nm}$,²⁶ and $\nu_0 = 5 \times 10^{12} \text{ s}^{-1}$. The results of the numerical calculation (eq 20) and the analytical formula (eq 24) are plotted in Figure 1b. We remark that both lines in Figure 1b (i) have exactly the same slope and (ii) differ by a small multiplicative factor (due to the approximations involved in eq 24), of about 3, that becomes larger as T_0 increases. Therefore, eq 24 is a good practical approximation. In addition, the absolute values of D_{n} are close to those obtained in the MT model, and hence, in agreement with the literature results. (The exact match between all of the lines in Figure 1b is coincidental because in MT the line can be shifted by changing the bulk value D_0 of TiO_2 .) This is a first indication that indeed the hopping model is a good candidate to describe the $D_{\text{n}}(E_{\text{F}})$ typically measured in DSC.

Further features of the hopping model concern the temperature dependence of transport quantities and are illustrated in Figure 3. According to eq 17, the transport level changes with the temperature, and for the assumed parameters the change is about 60 meV over 100 K, see Figure 3a. The effective “free electron” diffusion coefficient can be defined from eq 24 at $E_{\text{F}} = E_{\text{tr}}$ and has the value

$$D_0^{\text{hopping}} = \frac{9T_0^2}{4T^2} \left(\frac{T_0}{T} - 1 \right) e^{-3T_0/T} \alpha^2 \nu_0 \quad (26)$$

D_0^{hopping} also shows a temperature dependence as illustrated in Figure 3b. Thus, the intercept of $D_{\text{n}}(E_{\text{F}})$ lines at different temperatures, as shown in Figure 3c, does not indicate the transport level exactly, in contrast to MT. Still, in a first approximation the intercept shows roughly the position of E_{tr} , which is substantially below the conduction band level E_0 . Thus, we can appreciate that the model results in Figure 3b show good agreement with the experimental results of Figure 2c. The hopping model seems to describe this feature much better than the MT model.

We are therefore encouraged to fit the results in Figure 2c with the model of eq 24 in order to obtain the electronic parameters included in the hopping model. However, one must be careful when treating the $D_{\text{n}}(E_{\text{F}})$ data because, as mentioned above in the MT analysis, the slopes in the experimental data of Figure 2c only give the parameter T_0 (which can already be inferred from the capacitance). Each line has then only one degree of freedom (the prefactor), and we choose to fit $D_{\text{n}}(E_{\text{F}})$ using the above-mentioned parameters and leaving as the free parameter the position of the conduction band edge with respect to $E_{\text{redox}}(\text{I}^-/\text{I}_3^-)$, E_0 . From the lines in Figure 2c, we obtain the values $E_0^{273\text{K}} = 0.914 \text{ eV}$ and $E_0^{333\text{K}} = 0.884 \text{ eV}$. The two values differ by a small amount of about 30 meV, in agreement

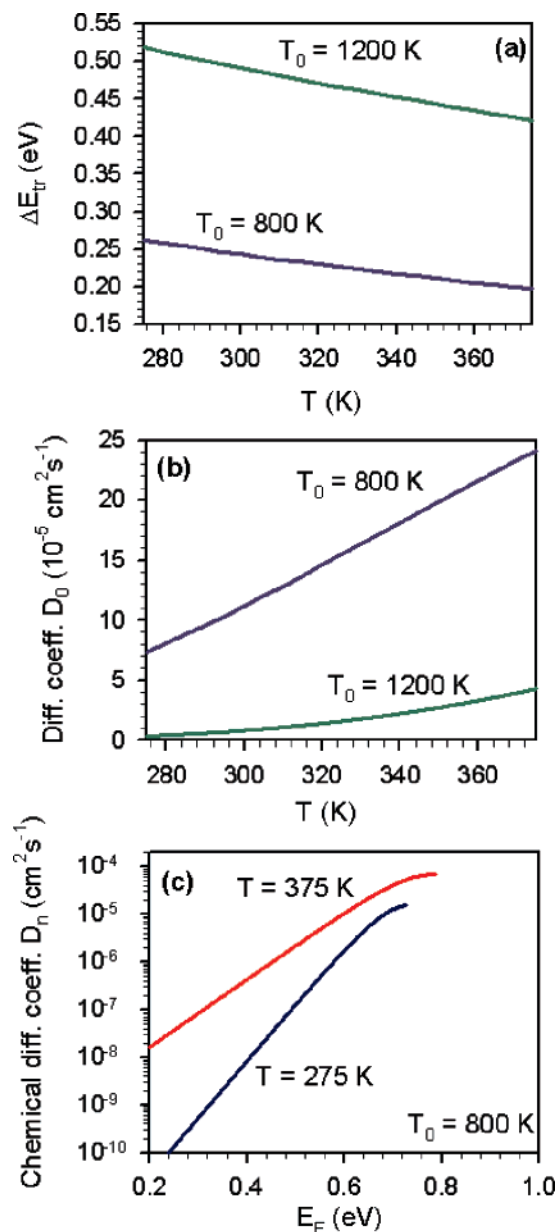


Figure 3. (a) Transport energy relative to the conduction band edge and the effective “free electron” diffusion coefficient D_0^{hopping} , as a function of temperature. (b) Chemical diffusion coefficient, calculated in the hopping model with the transport energy concept (for $E_F \leq E_{tr}$), with the numerical integration of the average jump frequency. The following parameters were used in the calculation: $E_0 = 1$ eV, $N_L = 10^{21} \text{ cm}^{-3}$, T_0 as indicated, $\alpha = 0.5$ nm, and $\nu_0 = 5 \times 10^{12} \text{ s}^{-1}$

with the stationary values of the capacitance. These values are furthermore reasonably close to those presented in the literature.^{21,22}

In comparison with previous literature calculations, we note that the Fermi-level dependence of the conductivity obtained in eq 25 is in agreement with the result of Vissenberg and Matters,²⁷ which was obtained using the critical path analysis based on percolation theory. Such analysis is more reliable than our simple approach that assumes from the start the activated hops to the transport energy.²⁸ Unfortunately, the percolation analytical approach does not provide the conductivity prefactor, and this prevents the comparison of our analytical results with those of the percolation framework. Therefore, concerning the absolute values of the hopping diffusion coefficient, our analytical results based on averaging the hopping rates must be

regarded as an estimation, and for further check of the validity of eqs 24 and 25 one should compare them with Monte Carlo simulations as discussed by Baranovskii et al.²⁸ This last paper also gives consideration of the contribution of the localized states between E_{tr} and E_0 to electron displacement. In addition, it should be emphasized that the transport energy approach does not work well when the Fermi level approaches the level E_{tr} . In fact, when the Fermi energy rises, the average distance between sites decreases rapidly and the tunneling becomes favorable over thermal activation to the higher energies. Therefore, diffusion in the high carrier density range requires a different approach.

Another work worth commenting on is that of Nelson et al.²⁹ These authors used a simulation method based on the continuous time random walk (CTRW) algorithm to compare multiple trapping and hopping transport in the interpretation of transient optical spectroscopy of the recombination of electrons with the dye cations in DSCs. However, the transition rates assumed in this paper are rather unconventional because the localization radius, which we termed here α , is energy-dependent in ref 29. This is not in agreement with the core, and almost universal, assumption of transition rates in hopping conductivity, indicated in eq 11, above, namely, that the energy dependence is only on the second term of the exponent of upward jumps, while the tunneling factor is independent of energy. Therefore the results in ref 29 are not claims about standard hopping theory and are not in conflict with ours. Using the standard Miller–Abrahams jump rates, the CTRW simulation of hopping should lead to a transport energy level quite similar to multiple trapping, as we have discussed above, and in more detail elsewhere.³⁰

It is well agreed that recombination in DSC is influenced by trapping effects. A model based on trapping and detrapping followed by interfacial charge transfer at the conduction band levels^{31,32} seems to be so far the best approach for the interpretation of electron lifetimes.³ In this approach, the same factors that affect the chemical diffusion coefficient of electrons determine the lifetime dependence on Fermi level. Therefore, it is obvious that the clarification of the interpretation of the transport level for electrons in the nanostructured metal oxides used in DSC can have a substantial impact on the understanding of recombination processes. This important question requires further work.

In conclusion, we have derived a useful working formula for the interpretation of the chemical diffusion coefficient of electrons in DSC using the hopping model. This approach seems to describe well some features of the data that are not captured correctly in the multiple trapping model, especially concerning the temperature dependence and energy levels governing electron transport. However, it must be recognized that the linear region of $\log D_n(E_F)$ contains very little information on the transport mechanism. We hope that the present considerations will encourage further experimental work in the temperature dependence and high carrier density regime, where the transport mechanism should be unambiguously identified. If the hopping model is confirmed by such measurements, then it can provide interesting new insight into the operation of dye-sensitized solar cells.

Acknowledgment. I am grateful to Volodia Kytin for many discussions on hopping transport. The work was supported by MEC projects MAT2004-05168 and HOPE CSD2007-00007 (Consolider-Ingenio 2010).

References and Notes

- (1) O’ Regan, B.; Grätzel, M. *Nature* **1991**, *353*, 737.
- (2) Bisquert, J. *J. Phys. Chem. B* **2004**, *108*, 2323.

- (3) Peter, L. M. *J. Phys. Chem. C* **2007**, *111*, 6601.
- (4) Bisquert, J. *Phys. Chem. Chem. Phys.*, DOI:10.1039/b709316k (2007).
- (5) Wang, Q.; Ito, S.; Grätzel, M.; Fabregat-Santiago, F.; Mora-Seró, I.; Bisquert, J.; Bosshoa, T.; Imaic, H. *J. Phys. Chem. B* **2006**, *110*, 19406.
- (6) O'Regan, B.; Durrant, J. R. *J. Phys. Chem. B* **2006**, *110*, 8544.
- (7) Kopidakis, N.; Benkstein, K. D.; van de Lagemaat, J.; Frank, A. J. *J. Phys. Chem. B* **2003**, *107*, 11307.
- (8) *Charge Transport in Disordered Solids with Applications to Electronics*; Baranovskii, S. D., Ed.; Wiley: Weinheim, 2006.
- (9) Grünewald, M.; Thomas, P. *Phys. Status Solidi B* **1979**, *94*, 125.
- (10) Monroe, D. *Phys. Rev. Lett.* **1985**, *54*, 146.
- (11) Shapiro, F. R.; Adler, D. *J. Non-Cryst. Solids* **1985**, *74*, 189.
- (12) Baranovskii, S. D.; Thomas, P.; Adriaenssens, G. J. *J. Non-Cryst. Solids* **1995**, *190*, 283.
- (13) Peter, L. M.; Walker, A. B.; Boschloo, G.; Hagfeldt, A. *J. Phys. Chem. B* **2006**, *110*, 13694.
- (14) Baranovskii, S. D.; Faber, T.; Hensel, F.; Thomas, P. *J. Phys.: Condens. Matter* **1997**, *9*, 2699.
- (15) Arkhipov, V. I.; Heremans, P.; Emelianova, E. V.; Adriaenssens, G. J.; Bäessler, H. *Appl. Phys. Lett.* **2003**, *82*, 3245.
- (16) Hartenstein, B.; Bäessler, H. *J. Non-Cryst. Solids* **1995**, *190*, 112.
- (17) Bisquert, J.; Fabregat-Santiago, F.; Mora-Seró, I.; Garcia-Belmonte, G.; Barea, E. M.; Palomares, E. *Inorg. Chim. Acta*, doi:10.1016/j.ica.2007.05.032 (2007).
- (18) Lobato, K.; Peter, L. M.; Wurfel, U. *J. Phys. Chem. B* **2006**, *110*, 16201.
- (19) O'Regan, B. C.; Durrant, J. R.; Sommeling, P. M.; Bakker, N. J. *J. Phys. Chem. C* **2007**, *111*, 14001.
- (20) Bisquert, J.; Cahen, D.; Rühle, S.; Hodes, G.; Zaban, A. *J. Phys. Chem. B* **2004**, *108*, 8106.
- (21) Lenzmann, F.; Krueger, J.; Burnside, S.; Brooks, K.; Grätzel, M.; Gal, D.; Rühle, S.; Cahen, D. *J. Phys. Chem. B* **2001**, *105*, 6347.
- (22) O'Regan, B. C.; Lenzmann, F. *J. Phys. Chem. B* **2004**, *108*, 4342.
- (23) Miller, A.; Abrahams, S. *Phys. Rev.* **1960**, *120*, 745.
- (24) Gomer, R. *Rep. Prog. Phys.* **1990**, *53*, 917.
- (25) Fabregat-Santiago, F.; Mora-Seró, I.; Garcia-Belmonte, G.; Bisquert, J. *J. Phys. Chem. B* **2003**, *107*, 758.
- (26) Mora-Seró, I.; Dittrich, T.; Belaidi, A.; Garcia-Belmonte, G.; Bisquert, J. *J. Phys. Chem. B* **2005**, *109*, 8035.
- (27) Vissenberg, M. C. J. M.; Matters, M. *Phys. Rev. B* **1998**, *57*, 12964.
- (28) Baranovskii, S. D.; Rubel, O.; Thomas, P. *Thin Solid Films* **2005**, *487*, 2.
- (29) Nelson, J.; Haque, S. A.; Klug, D. R.; Durrant, J. R. *Phys. Rev. B* **2001**, *63*, 205321.
- (30) Anta, J. A.; Mora-Seró, I.; Dittrich, T.; Bisquert, J. To be submitted for publication.
- (31) Bisquert, J.; Vikhrenko, V. S. *J. Phys. Chem. B* **2004**, *108*, 2313.
- (32) Bisquert, J.; Zaban, A.; Greenshtein, M.; Mora-Seró, I. *J. Am. Chem. Soc.* **2004** *126*, 13550.